Incomplete accumulation of perilesional reactive astrocytes exacerbates wound healing after closed-head injury by increasing inflammation and BBB disruption

Sawant, Nitin
Watanabe, Airi
Ueda, Haruna
Okano, Hideyuki
Morita, Mitsuhiro

(Citation)
Experimental Neurology,374:114700

(Issue Date)
2024-04

(Resource Type)
journal article

(Version)
Version of Record

Experimental Neurology 374 (2024) 114700

Contents lists available at ScienceDirect

Experimental Neurology

journal homepage: www.elsevier.com/locate/yexnr

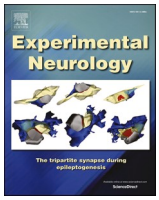

Research paper

Incomplete accumulation of perilesional reactive astrocytes exacerbates wound healing after closed-head injury by increasing inflammation and BBB disruption

Nitin Sawant [a], Airi Watanabe [a], Haruna Ueda [a], Hideyuki Okano [b], Mitsuhiro Morita [a,c,*]

[a] Biomolecular Organization, Department of Biology, Kobe University, Kobe, Hyogo 657-8501, Japan
[b] Department of Physiology, Keio University School of Medicine, Tokyo 160-8582, Japan
[c] Application Division, Center of Optical Scattering Image Science, Kobe University, Kobe, Hyogo 657-8501, Japan

ARTICLE INFO

Keywords:
Brain injury
Reactive astrocyte
Wound healing
Inflammation
Blood brain barrier
STAT3

ABSTRACT

Wound healing after closed-head injury is a significant medical issue. However, conventional models of focal traumatic brain injury, such as fluid percussion injury and controlled cortical impact, employ mechanical impacts on the exposed cerebral cortex after craniotomy. These animal models are inappropriate for studying gliosis, as craniotomy itself induces gliosis. To address this, we developed a closed-head injury model and named "photo injury", which employs intense light illumination through a thinned-skull cranial window. Our prior work demonstrated that the gliosis of focal cerebral lesion after the photo injury does not encompass artificial gliosis and comprises two distinct reactive astrocyte subpopulations. The reactive astrocytes accumulated in the perilesional recovery area actively proliferate and express Nestin, a neural stem cell marker, while those in distal regions do not exhibit these traits. The present study investigated the role of perilesional reactive astrocytes (PRAs) in wound healing using the ablation of reactive astrocytes by the conditional knockout of *Stat3*. The extensive and non-selective ablation of reactive astrocytes in *Nestin-Cre:Stat3*$^{f/f}$ mice resulted in an exacerbation of injury, marked by increased inflammation and BBB disruption. On the other hand, *GFAP-CreER*^{T2}*:Stat3*$^{f/f}$ mice exhibited the partial and selective ablation of the PRAs, while their exacerbation of injury was at the same extent as in *Nestin-Cre:Stat3*$^{f/f}$ mice. The comparison of these two mouse strains indicates that the PRAs are an essential astrocyte component for wound healing after closed-head injury, and their anti-inflammatory and regenerative functions are significantly affected even by incomplete accumulation. In addition, the reporter gene expression in the PRAs by *GFAP-CreER*^{T2} indicated a substantial elimination of these cells and an absence of differentiation into other cell types, despite Nestin expression, after wound healing. Thus, the accumulation and subsequent elimination of PRA are proposed as promising diagnostic and therapeutic avenues to bolster wound healing after closed-head injury.

1. Introduction

There is a significant societal and medical need to improve wound healing after closed-head injuries due to falls, traffic accidents, and sports injuries (Maas et al., 2017). Since focal intact skull cerebral lesions are common in these brain injuries, we have developed a novel brain injury model and named "photo injury", which is created by intense light illumination through a thinned-skull cranial window (Suzuki et al., 2012). This light illumination increases the tissue temperature by a few degrees at the focus and forms a cerebral contusion within one month (Suzuki et al., 2012), presumably through heat-induced hyperexcitability (Das et al., 2021) and subsequent dysregulation of glucose metabolism, which is a common degenerative process in the acute phase of head trauma (Amorini et al., 2016; Koenig and Dulla, 2018). Mechanical impacts on the skull often result in focal cerebral lesions in large human brains, with no damage to the life-sustaining brainstem. However, the force of mechanical impact is hardly adjusted to induce cerebral lesions in small rodent brains without affecting the brainstem. Therefore, conventional traumatic brain injury models, such as fluid percussion injury and controlled cortical impact (CCI), employ mechanical impacts on the exposed cerebral cortex after craniotomy. These brain injury models are inappropriate to study gliosis, as

* Corresponding author at: Department of Biology, Kobe University, 1-1 Rokkodai Nada, Kobe, Hyogo 657-8501, Japan.
E-mail address: mmorita@boar.kobe-u.ac.jp (M. Morita).

https://doi.org/10.1016/j.expneurol.2024.114700
Received 15 October 2023; Received in revised form 17 January 2024; Accepted 22 January 2024
Available online 23 January 2024

craniotomy itself induces gliosis (Xu et al., 2007). Meanwhile, the thinned-skull cranial window does not induce the activation of astrocytes and microglia (Xu et al., 2007), and our photo injury does not encompass artificial gliosis (Suzuki et al., 2012). Therefore, our photo injury offers a unique opportunity to explore how gliosis influences the outcome of closed-head injury.

Our previous report showed that the photo injury is followed by a prominent perilesional tissue recovery. Furthermore, the reactive astrocytes in the perilesional recovery area actively proliferate and express Nestin, a neural stem cell marker, whereas those in distal regions lacked both traits (Suzuki et al., 2012). While similar perilesional reactive astrocytes (PRAs) have been highlighted in several publications, their role in the pathological process after injury remains a subject of debate. The ablation of perilesional Nestin-expressing reactive astrocytes after spinal cord injury by conditional *Stat3* knockout with *Nestin-Cre* exacerbated injury (Okada et al., 2006; Renault-Mihara et al., 2017). The reactive astrocytes in the vicinity of various brain lesions acquire stem cell properties, which are thought to accelerate wound healing by replenishing cells lost due to injury (Sirko et al., 2013). In contrast to these beneficial influences of PRAs, the suppression of proliferating reactive astrocytes after CCI by conditional *Sox2* knockout with *Gfap-CreER*^{T2} reduced lesion size and improved behavioral recovery (Chen et al., 2019). The ablation of proliferating reactive astrocytes exacerbated moderate CCI, which has minimum inflammation, but did not affect severe CCI, which has significant inflammation (Myer et al., 2006). Thus, the accumulation and functions of PRAs are likely influenced by the context of injury. Such a complexity is supposed to reflect the diversity of reactive astrocytes, which is suggested by our previous *in vitro* studies showing the dual regulation of astrocyte functions by growth factors and proinflammatory cytokines (Morita et al., 2003, 2007), as well as the recent identification of neurodegenerative A1 and neuroprotective A2 reactive astrocyte subtypes (Liddelow et al., 2017). Thus, the PRAs after closed-head injury remain to be characterized as future diagnostic and therapeutic avenues.

In order to address this issue, we ablated reactive astrocytes after the photo injury by conditional knockout of *Stat3*. Signal Transducer and Activator of Transcription 3 (STAT3) is a common transcription factor for inducing both A1 and A2 reactive astrocytes (Fan and Huo, 2021), and conditional *Stat3* knockout has previously been shown to ablate reactive astrocytes (Okada et al., 2006; Nobuta et al., 2012; Reichenbach et al., 2019). In the present study, we found that the ablation was extensive and non-selective for both reactive astrocyte subpopulations in *Nestin-Cre:Stat3*$^{f/f}$ mice (Nes-STAT3 mice), while partial and PRA-selective in *Gfap-CreER*^{T2}*:Stat3*$^{f/f}$ mice (GFAP-STAT3 mice). Therefore, we investigated the role of PRAs in wound healing through the histological comparison of these mice. In addition, we also examined the fate of PRAs by the PRA-selective reporter gene expression using *GFAP-CreER*^{T2}, because the PRAs are thought to acquire stem cell properties, as indicated by Nestin expression. Our data demonstrate the essential role of PRAs after closed head injury.

2. Materials and methods

2.1. Animal experiments

All animal experiments were approved by the Institutional Animal Care and Use Committee of Kobe University (approval number: 24–01, 28–06-06) and conducted in accordance with the Animal Experimentation Regulations of Kobe University. Mice were housed in cages with unrestricted access to food pellets and water and maintained in an environment with controlled temperature (23 ± 2 °C), humidity (50 ± 10%), and 12 h light/dark cycle. All mice were of C57BL/6 J background, including wild type mice used as controls. *Nestin-Cre:Rosa26-GFP* mice (Nes-GFP mice) and *Nestin-Cre:Stat3*$^{f/f}$ mice (Nes-STAT3 mice) were generated by crossing *Nestin-Cre* mice (Okada et al., 2006) with *Rosa26-GFP* mice (Kawamoto et al., 2000) and *Stat3*$^{f/f}$ mice (Okada et al., 2006), respectively. *Gfap-CreER*^{T2}*:Rosa26-GCaMP6* mice (GFAP-GCaMP mice) and *Gfap-CreER*^{T2}*:Stat3*$^{f/f}$ mice (GFAP-STAT3 mice) were generated by crossing *Gfap-CreER*^{T2} mice (Hirrlinger et al., 2006) with *Rosa26-GCaMP6* mice (RIKEN BRC RBRC09450) (Ohkura et al., 2012) and *Stat3*$^{f/f}$ mice, respectively. The photo injury was generated in 8–16 weeks old mice of both sexes as described (Suzuki et al., 2012). Briefly, each mouse was anesthetized with ketamine (100 mg/kg, Daiichi-Sankyo, Tokyo, Japan) and xylazine (10 mg/kg, Bayer Yakuhin, Osaka, Japan) and a thinned-skull cranial window (~ 0.5 mm in diameter and ~ 20 μm in thickness) was created over the right primary somatosensory cortex (1.5 mm posterior to the bregma and 3 mm lateral from the midline) by scraping the skull with a micro-drill burrs (19007-07 M; FST, Foster City, CA, USA) and a microsurgical blade (Nordland Blade #6900; Salivan, Charlotte, NC, USA). The mouse was mounted on a microscope stage for light illumination. Its head was fixed with the cranial window centered under a 20× water immersion microscope objective (XLUMPLFLN 20× W NA1.0; Olympus, Tokyo, Japan), setting the focal point 200 μm below the cortical surface. The cortical tissue was exposed for a duration of 1.5–2.5 min to the light from a 90-W halogen bulb mounted in a housing directly over a microscope camera port. We adjusted the exposure time at every bulb replacement to ensure the induction of total neuronal loss, reaching 80–90% of the cortical thickness within 12 h after exposure. Tamoxifen (Toronto Research Chemicals, Toronto, Canada) dissolved in corn oil (Sigma-Aldrich, St. Louis, MO, USA) was administered orally (250 mg/kg) one day before the photo injury.

2.2. Immunofluorescence analysis

Mice were sacrificed at specified time points after injury and tissue samples were subjected to histological analysis. After anesthesia with an overdose of sodium pentobarbital (75 mg/ kg, i.p.), mice were transcardially perfused with ice-cold 0.1 M PBS containing 1 units/mL heparin (Wako, Tokyo, Japan), followed by 4% (*w/v*) paraformaldehyde in 0.1 M phosphate-buffered saline (PBS). Brains were postfixed for six hours and sliced coronally at a thickness of 100 μm in PBS using a microslicer (Zero-One, DOSAKA, Osaka, Japan). The slices were stored at −20 °C in a preservative containing 0.3% glycerol, 0.3% ethylene glycol, 0.1 M sodium phosphate, and 0.85% NaCl. For immunofluorescence staining, the slices were washed with PBS, twice, 10 min each, treated with 50 mM NH4Cl for 10 min, washed with PBS, twice, 10 min each, permeabilized with PBS containing 0.4% (w/v) Triton X-100 for two hours, and blocked with blocking buffer (PBS containing 5% normal goat serum and 0.1% Triton X-100). Slices were incubated with primary antibodies in blocking buffer overnight at 4 °C, returned to room temperature, washed with PBS, three times, 10 min each, incubated with secondary antibodies in blocking buffer for two hours, washed with PBS, three times, 10 min each, and mounted with Gelvatol (Harlow and Lane, 2006) containing 100 mg/mL DABCO (Sigma). Primary antibodies included: rabbit anti-GFAP (1:250, Vector Laboratories); mouse anti-NeuN (1:500, CHEMICON); rat anti-CD68 (1:300, abcam); rabbit anti-Stat3 (1:500, Sigma); rabbit anti-Iba1 (1:200, Wako); rabbit GFP (1:500, Invitrogen); mouse anti-S100β (1:400, DAKO, Glostrup, Denmark). Immunofluorescence was visualized with FITC-, Cy3- or Cy5-conjugated secondary antibodies (1:100, Jackson ImmunoResearch Laboratories, West Grove, PA, USA). Low magnification fluorescence images of Nissl staining were obtained by an epifluorescence microscope (IX70, Olympus) equipped with a 2× Objective and a cooled-CCD camera (Orca-ER, Hamamatsu, Hamamatsu, Japan). Other fluorescence images were obtained as *Z*-stacks of confocal images (step size = 2 μm) using a Fluoview1000 (Olympus) with a 20× or 40× objectives and analyzed using Fiji (Schindelin et al., 2012).

2.3. Quantitative analysis

The densities of cells and GFAP fibers, as well as IgG fluorescence,

were measured in region of interest (ROI), which were total 0.1–0.2 mm^2 from each mouse. GFAP fibers were measured as total number of pixels above the predetermined threshold of fluorescence intensity, which was consistently set for all sample. IgG deposition was measured as the average digitized fluorescence intensity in ROI. Statistical analysis was conducted by Microsoft Excel, and graphs were generated by Matplotlib (Hunter, 2007). Data were expressed as the mean ± standard deviation of the mean (SD) with dots representing individual mice. The number of mice subjected to analysis was indicated by 'n' in each figure legend. Difference between groups were assessed using two-tailed Student's test-test. Significance was set at $P < 0.05$.

3. Results

3.1. STAT3 activation in astrocytes after injury was abolished in Nes-STAT3 mice

It has been shown that the reporter gene expression and conditional knockout by *Nestin-Cre* are selective for perilesional Nestin+ reactive astrocytes after spinal cord injury, in a series of reports (Okada et al., 2006; Renault-Mihara et al., 2017). Meanwhile, this mouse strain is widely used to label or manipulate neural stem cells during development and their progeny, including adult neurons and astrocytes (Gavériaux-Ruff and Kieffer, 2007). Therefore, the efficiency of *Nestin-Cre* for cerebral neurons and astrocytes, as well as for reactive astrocytes at 7 days post-injury (dpi) was examined using Nes-GFP mice. As shown in Fig. 1A and B, GFP expression was induced in 62% of astrocytes (S100β+), whereas it was 32% and 0% in neurons (NeuN+) and microglia (Iba1+), respectively. Meanwhile, the efficiency for the PRAs (GFAP+) was 84%, indicating an increase in efficiency for astrocytes after injury (Fig. 1C and D). These results suggest that Stat3 is deleted in both normal cortical neurons and astrocytes, and additionally in the PRAs after injury in Nes-STAT3 mice. *Stat3* is essential for the differentiation of neural stem cells into astrocytes (Herrmann et al., 2008), which play a vital role in maintaining the brain environment (Götz et al., 2015). However, no significant differences were observed in the distribution and morphology of cerebral neurons, astrocytes and microglia, as well as in the limited GFAP expression between the control (Cont) and Nes-STAT3 mice (Fig. 2A and B). In addition, the densities of neurons, astrocytes and microglia did not significantly differ between Cont and Nes-STAT3

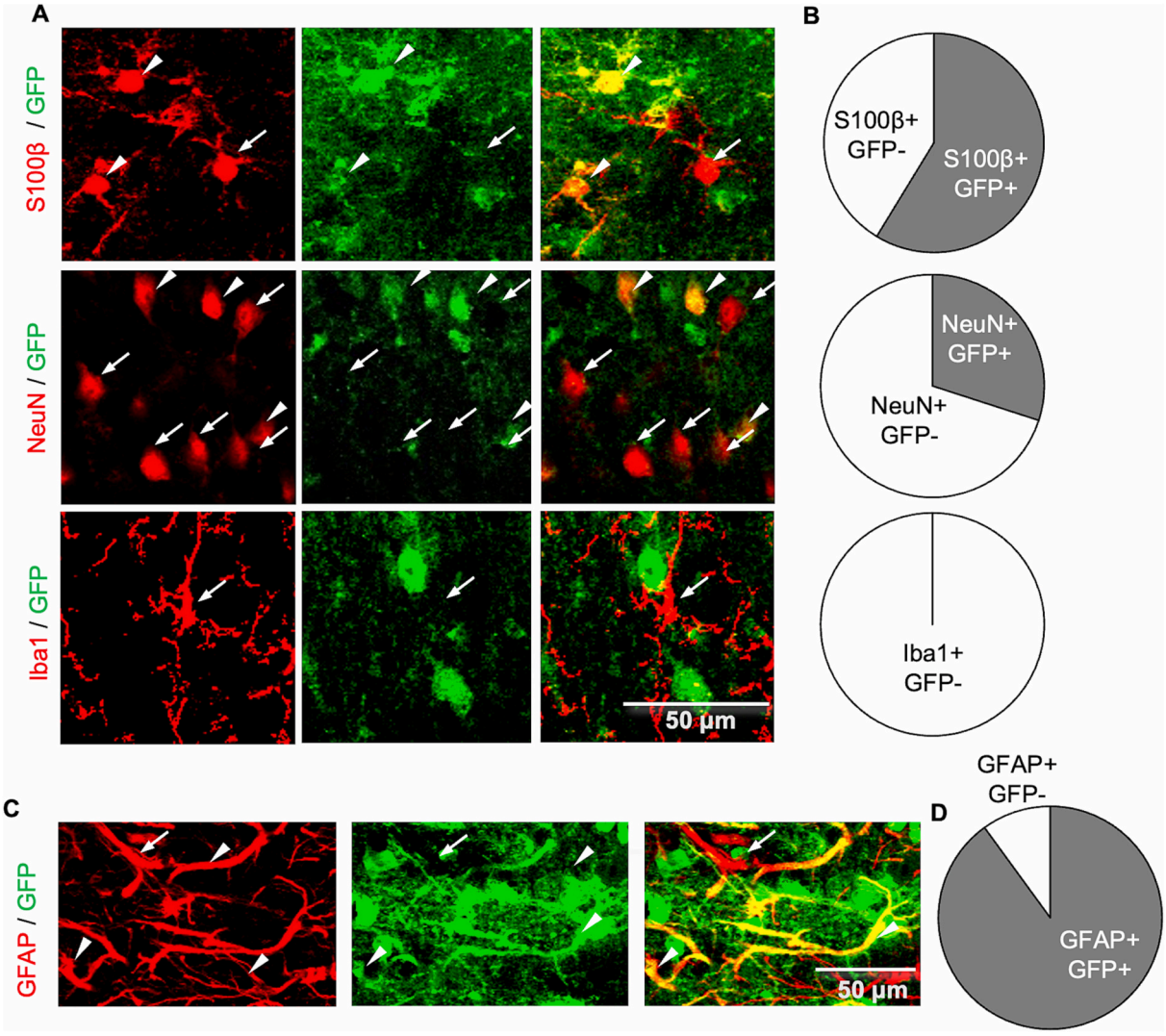

Fig. 1. Reporter gene expression was induced in both cortical neurons and astrocytes before injury, and additionally in the PRAs after injury in Nes-GFP mice. Immunostaining images of reporter gene (GFP) and markers for astrocytes (S100β), neurons (NeuN) and microglia (Iba1) (A) and recombination efficiency in astrocytes (S100β+), neurons (NeuN+) and microglia (Iba1+) (B) in the cerebral cortex of *Nestin-Cre:Rosa26-GFP* (Nes-GFP) mice ($n = 3$, total 90 cells for each marker). Cell type marker-positive cells with and without reporter gene expression are indicated by arrows and arrowheads, respectively, in (A). Immunostaining of GFP and a reactive astrocyte marker (GFAP) (C), and the recombination efficiency in reactive astrocytes (GFAP+) (D) in the perilesional region of Nes-GFP mice at 7 days post-injury (dpi) (n = 3, total 90 cells).

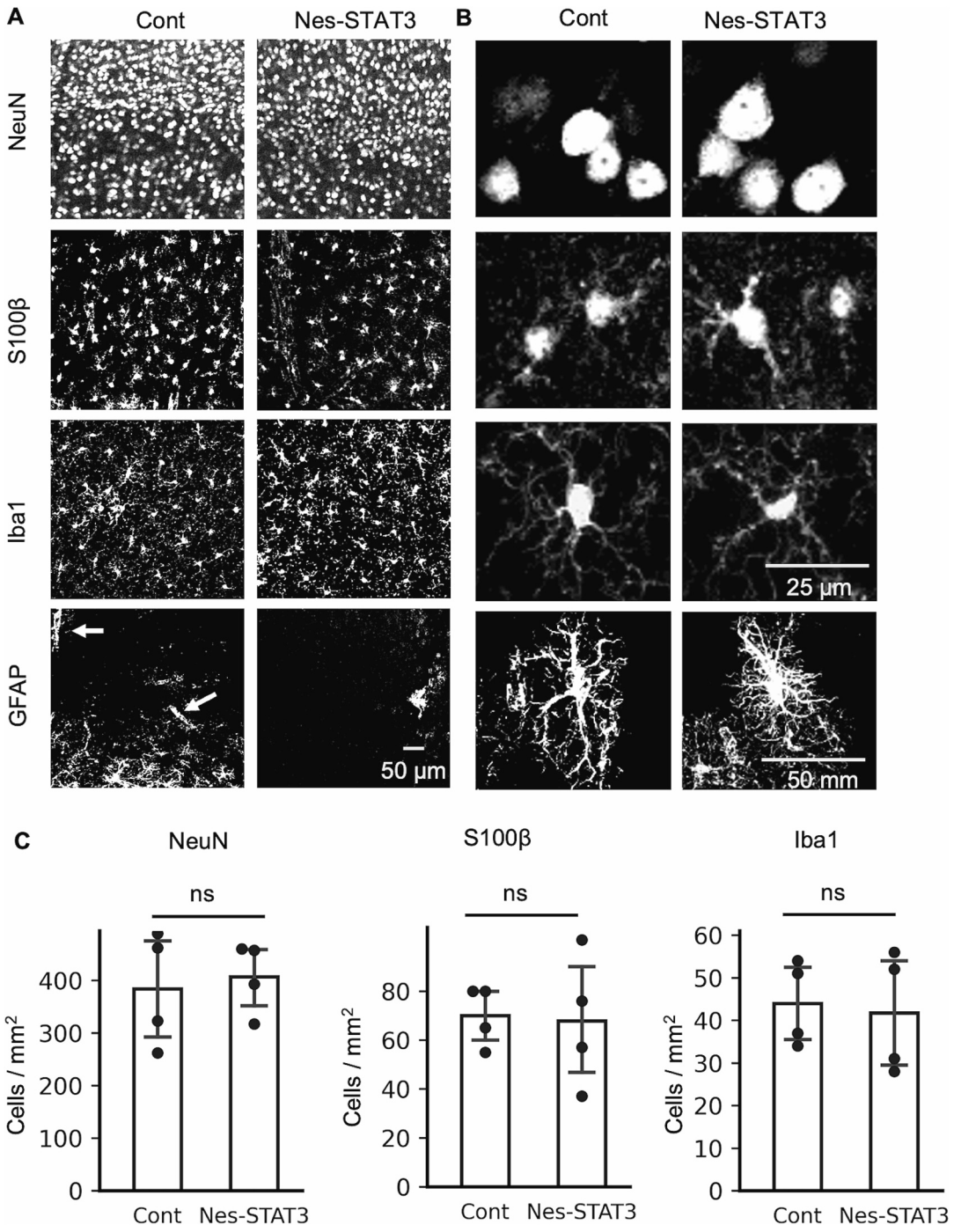

Fig. 2. Distribution, morphology and density of neurons, astrocytes and microglia were not significantly different between control and Nes-STAT3 mice.
Low (A) and high (B) magnification images of NeuN, S100β, Iba1 and GFAP immunostaining, and the densities of neurons (NeuN), astrocytes (S100β) and microglia (Iba1) (C) in the cerebral cortex of control (Cont, $n = 4$) and *Nestin-Cre:Stat3*$^{f/f}$ (Nes-STAT3, n = 4) mice. Mean ± SD. ns, not significant by Student's *t*-test. The arrows in (A) indicate clusters of GFAP+ cells along large blood vessels.

mice (Fig. 2C). The density of GFAP+ cells was not measured because it is too low and significantly fluctuates depending on the cortical areas, primarily due to the presence of clusters of GFAP+ cells along large blood vessel (Fig. 2A, arrows). On the other hand, the accumulation of STAT3 in the nuclei of GFAP+ reactive astrocytes after injury was largely abolished in both the perilesional (PR) and distal (DR) regions at 7 dpi in Nes-STAT3 mice (Fig. 3A). The densities of GFAP+/STAT3+ cells in the PR (15.3 ± 5.8 cells/mm^2) and DR (9.0 ± 1.0) of Nes-STAT3 mice were 88% and 85% significantly lower than in the PR (134.3 ± 42.7) and DR (59.3 ± 11.0) of Cont mice, respectively (Fig. 3B). These results indicate that STAT3 is activated exclusively in astrocytes after injury, and this STAT3 activation was largely abolished in Nes-STAT3 mice. The exclusive activation of STAT3 in astrocytes suggests that the deletion of Stat3 in non-astrocytic cells, including neurons, has a limited impact on the pathology after injury. Thus, the similarity of brain cells between Cont and Nes-STAT3 mice before injury, along with the abolition of astrocyte-selective STAT3 activation after injury in Nes-STAT3 mice, suggest that the difference between Cont and Nes-STAT3 after injury is primarily due to the extensive and non-selective ablation of reactive astrocytes resulting from the STAT3 abolition. It is

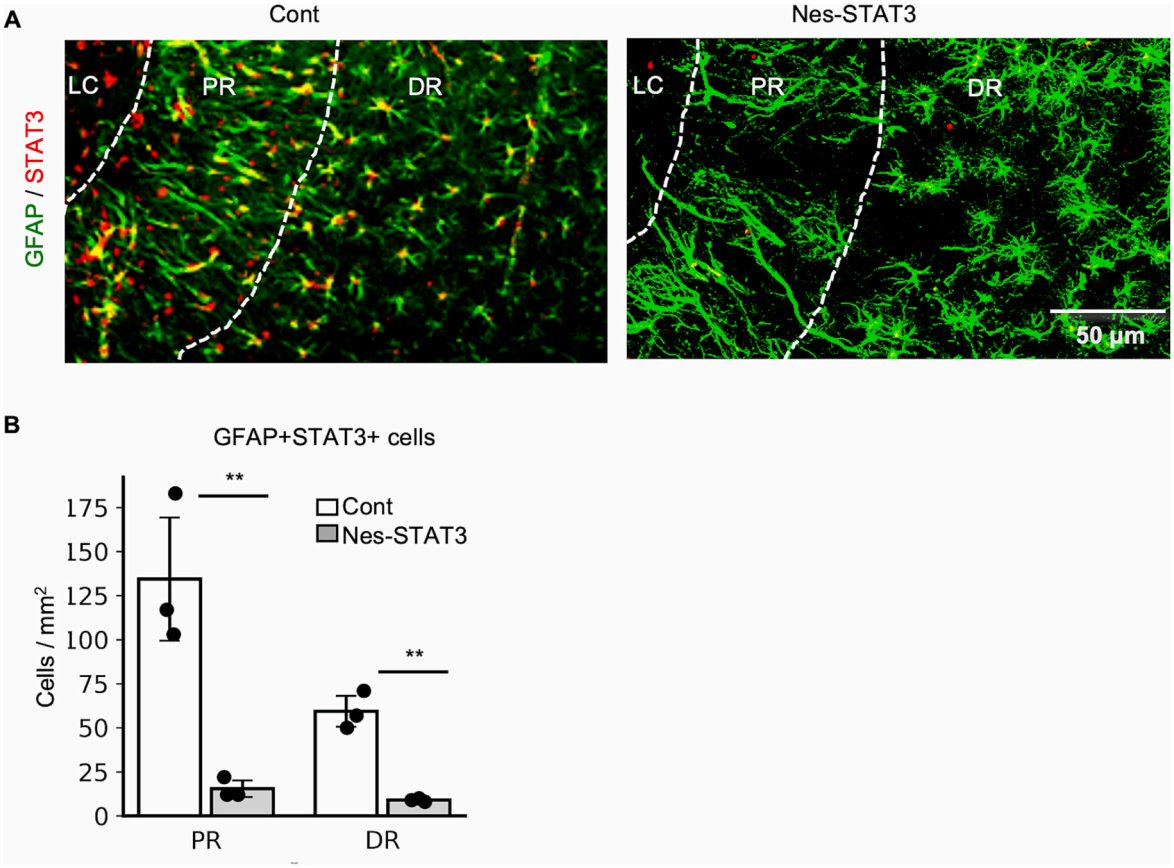

Fig. 3. Astrocyte-selective activation of STAT3 after injury was abolished in Nes-STAT3 mice.
GFAP and STAT3 immunostaining images (A) and the density of GFAP+/STAT3+ cells (B) in the cerebral cortex of Cont (n = 3) and Nes-STAT3 mice (n = 3) at 7 dpi. The boundaries between lesion core (LC), perilesional (PR) and distal (DR) regions are indicated by white dashed lines. Mean ± SD. $^{**}p < 0.01$, Student's t-test.

noteworthy that some reactive astrocytes lacking nuclear STAT3 accumulation in Nes-STAT3 mice (Fig. 3A right) are larger than those in Cont (Fig. 3A left). These characteristics of reactive astrocytes are supposed to reflect astrocyte activation in the absence of STAT3 signaling or in the perilesional region with impaired wound healing, as mentioned later.

3.2. *Extensive and non-selective ablation of reactive astrocytes exacerbate injury by accelerating inflammation and BBB disruption in Nes-STAT3 mice*

The ablation of reactive astrocytes and its impact on wound healing in Nes-STAT3 mice at 7 dpi were investigated. The size of lesion core (LC) visualized by Nissl staining in Nes-STAT3 mice (404.7 ± 25.9 A.U.) was 27% significantly larger than that in Cont mice (316.83 ± 29.10) (Fig. 4A and B). The density of GFAP+ fibers in both the PR (5.99 ± 0.82 A.U.) and DR (2.79 ± 1.07) of Nes-STAT3 mice was 82% and 84% significantly lower than that in the PR (33.77 ± 6.28) and DR (17.81 ± 5.32) of Cont mice (Fig. 4C and D). The remaining GFAP+ reactive astrocytes in Nes-STAT3 mice likely reflect the 84% recombination efficacy of Nestin-Cre in reactive astrocytes, as described for Fig. 1D. However, the contribution of GFAP+ cells in uninjured mice, as shown in Fig. 1A and B, and the STAT3-independent activation, as mentioned for Fig. 3 cannot be excluded. The density of perilesional Nissl+ neurons in Nes-STAT3 mice (73.66 ± 14.57 cells/mm^2) was 72% significantly lower than that in Cont mice (261.66 ± 40.46) (Fig. 4E). These results indicate that the extensive ablation of both perilesional and distal reactive astrocytes exacerbated injury, as reflected by LC size and perilesional neuronal density in Nes-STAT3 mice. In addition, the ablation of reactive astrocytes in Nes-STAT3 mice likely impaired perilesional tissue recovery, a process evidenced by the reduction of LC size and the expansion of perilesional region containing disorganized neurons, between 4 and 7 dpi in our previous study (Suzuki et al., 2012).

The impact of extensive and non-selective reactive astrocyte ablation was further analyzed with a focus on inflammation and BBB disruption. The density of perilesional CD68+ microglia in Nes-STAT3 mice (198.3 ± 26.6) was 137% significantly greater than in Cont (83.5 ± 13.5) (Fig. 5A and B). Similarly, the fluorescence intensity indicating perilesional IgG deposit in Nes-STAT3 mice (55.3 ± 19.0) was 368% significantly greater than in Cont mice (11.8 ± 5.8) (Fig. 5C and D). According to our previous study, the number of CD68+ microglia increases from 4 dpi to 7dpi, whereas IgG deposition at 4 dpi is largely cleared by 7 dpi in the PR (Suzuki et al., 2012). Therefore, these results suggest the accelerated accumulation of CD68+ microglia and impaired clearance of IgG, likely resulting from increased inflammation and BBB disruption, respectively, in Nes-STAT3 mice.

3.3. *PRA-specific inducible recombination with Gfap-CreERT2*

We examined several *Cre* driver mouse strains for PRA-selective knockout and found a PRA-selective recombination by *Gfap-CreER^{T2}*. GFAP-GCaMP mice were treated with tamoxifen one day before the photo injury and then reporter gene expression at 7 dpi was examined by GFP immunofluorescence staining. As shown in Fig. 6A, the majority of GFP+ cells were PRAs. The density of GFP+ cells in the PR (11.25 ± 2.87) was significantly higher than that in the DR (1.75 ± 1.70), and GFP+ cells in the DR were almost negligible (Fig. 6B). These results suggest that GFAP-STAT3 allows a PRA-selective ablation.

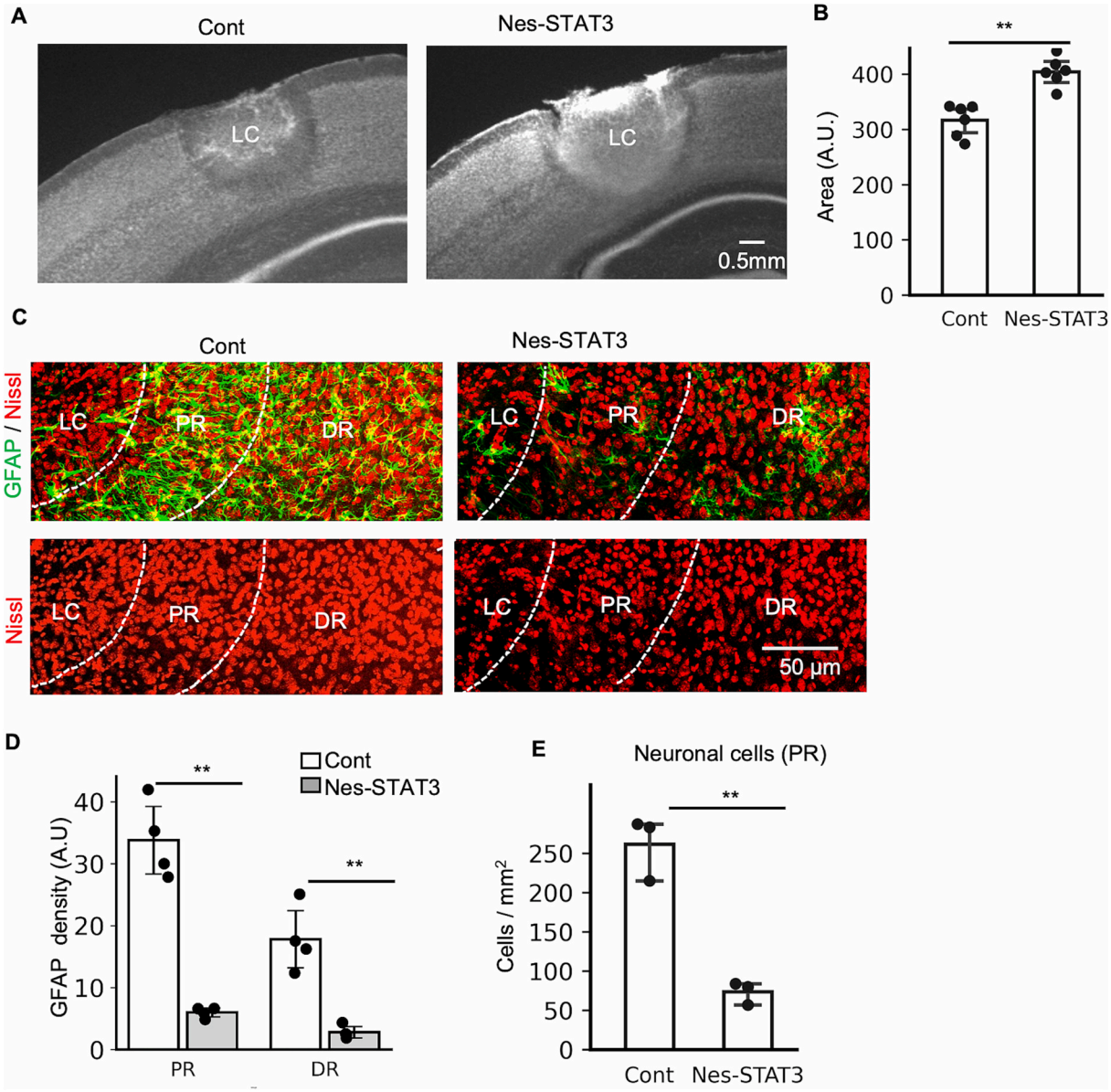

Fig. 4. Extensive and non-selective ablation of reactive astrocytes exacerbated injury in Nes-STAT3 mice.
Low magnification Nissl staining images of injury (A) and LC size (B) in Cont and Nes-STAT3 mice at 7 dpi. High magnification images of GFAP immunostaining and Nissl staining (C) and the density of GFAP+ fibers in the PR or DR (D) or Nissl+ neurons in the PR (E) in Cont (n = 4 for D and n = 3 for E) and Nes-STAT3 mice (n = 4 for D and n = 3 for E) at 7 dpi. Mean ± SD. **p < 0.01, Student's t-test.

3.4. Partial PRA ablation exacerbated injury by increasing inflammation and BBB disruption in GFAP-STAT3 mice

The ablation of PRAs and its impact on wound healing in GFAP-STAT3 mice at 7 dpi were investigated. The influence of tamoxifen was excluded by treating control mice with tamoxifen as for GFAP-STAT3. The size of LC in GFAP-STAT3 mice (412.6 ± 58.2) was 40% significantly larger than that in Cont mice (294.6 ± 28.2) (Fig. 7A and B). In the PR, the density of GFAP+ fibers in GFAP-STAT3 mice (20.1 ± 2.9) was 45% significantly lower than that in Cont mice (36.5 ± 8.3). However, in the DR, the density in GFAP-STAT3 mice (11.80 ± 2.60) was not significantly different from that in Cont mice (16.03 ± 2.31) (Fig. 7C and D). This indicates that the ablation of reactive astrocytes in GFAP-STAT is partial and selective to PRAs. The density of perilesional Nissl+ neurons in GFAP-STAT3 (155.7 ± 31.0) was 53% significantly lower than control (335.3 ± 46.4) (Fig. 7E). The exacerbation of injury was further analyzed with a focus on inflammation and BBB disruption. The density of perilesional CD68+ microglia in GFAP-STAT3 mice (171.0 ± 20.7) was 86% significantly greater than in Cont mice (91.5 ± 13.6) (Fig. 8A and B). Similarly, the fluorescence intensity indicating perilesional IgG deposit in GFAP-STAT3 mice (24.8 ± 12.3) was 211% significantly greater than in Cont mice (7.9 ± 5.4) (Fig. 8C and D). These results indicate that the partial and selective ablation of PRA in GFAP-STAT3 exacerbated the injury to a similar extent as the extensive and non-selective ablation of reactive astrocytes in the Nes-STAT3. In addition, the exacerbations of injury in GFAP-STAT3 and Nes-STAT3 likely result from a similar increase of inflammation and BBB disruption.

3.5. Elimination of PRAs after wound healing

In our previous study, the reduction of LC size saturated at 30 dpi (Suzuki et al., 2012), presumably due to the completion of wound healing. Thus, the fate of PRAs after wound healing was examined by comparing the GFAP and GFP immunostaining in GFAP-GCaMP6 mice

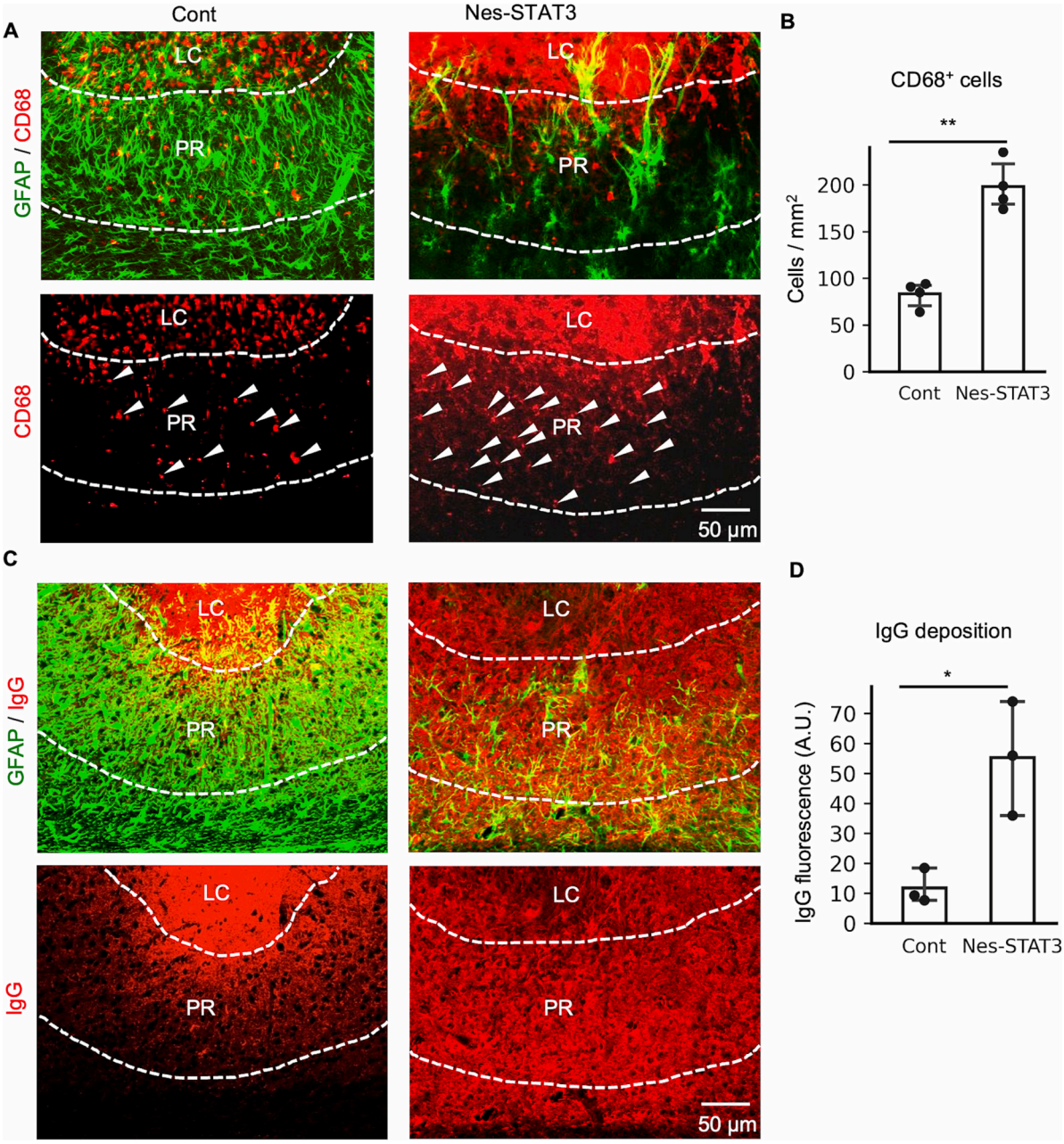

Fig. 5. Increased inflammation and BBB disruption in Nes-STAT3 mice.
GFAP and CD68 immunostaining images (A) and the density of CD68+ cells in the PR (B) in Cont and Nes-STAT3 mice at 7 dpi. Arrowheads indicate CD68+ cells in the PR in (A). GFAP and IgG immunostaining images (C) and the intensity of IgG immunofluorescence in the PR (D) in Cont (n = 3) and Nes-STAT3 (n = 3) mice at 7 dpi. Mean ± SD. **p < 0.01, *p < 0.05, Student's t-test.

at 7 dpi and 56 dpi (Fig. 9A and B). The density of GFAP+ fibers at 56 dpi (8.62 ± 2.69) was 70.9% significantly lower than that at 7 dpi (29.59 ± 7.03) in the PR. In addition, the majority of GFP+ cells were GFAP+ and GFP+/GFAP- cells were negligible at both 7 dpi and 56 dpi as shown in Fig. 9C. These results indicate that the PRAs are largely eliminated and persist as reactive astrocytes after wound healing.

4. Discussion

The role of PRAs in wound healing after closed head injury was investigated by ablating reactive astrocytes after the photo injury. Based on a series of preceding studies involving the ablation of PRAs in Nes-STAT3 mice after spinal cord injury (Okada et al., 2006; Renault-Mihara et al., 2017), we initially examined the efficiencies of *Nestin-Cre* after the photo injury. Nes-GFP mice showed reporter gene expressions in both normal cortical neurons and astrocytes, as well as in the PRAs. Meanwhile, Nes-STAT3 mice, whose brain cells were indistinguishable from control mice, showed the abolition of astrocyte-selective STAT3 activation. Thus, Nes-STAT3 mice were suggested as a model for studying the influences of extensive and non-selective ablation of reactive astrocytes on wound healing. In addition, we established a condition for PRA-selective recombination by *Gfap-CreER*^{T2}. GFAP-GCaMP showed a reporter gene expression specifically in the PRAs and the ablation in GFAP-STAT3 was partial and selective to the PRAs. Nes-STAT3 (82% ablation of PRAs) and GFAP-STAT3 (45% ablation of PRAs) showed similar exacerbation of injury with increased LC size (27% and 42% increases in Nes-STAT3 and GFAP-STAT3, respectively) and decreased density of perilesional neurons (72% and 52% decreases).

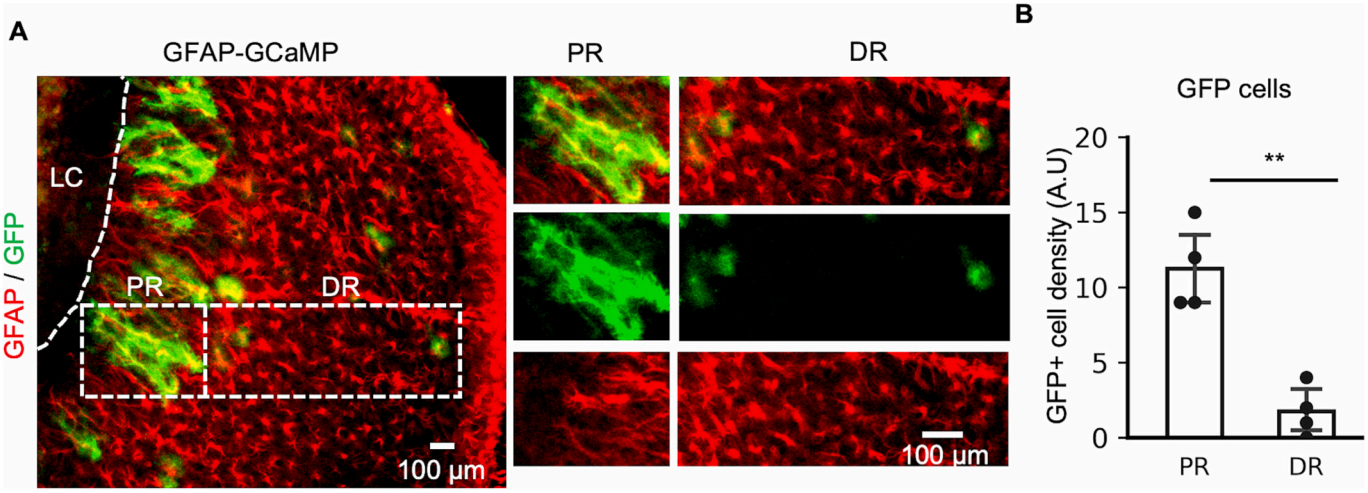

Fig. 6. Perilesional reactive astrocyte selective recombination by Gfap-CreERT2.
GFP and GFAP immunostaining images (A) and the densities of GFP+ cells (B) in the PR and DR of *Gfap-CreER^{T2}:Rosa26-GCaMP6* (GFAP-GCaMP, n = 4) mice at 7 dpi. Mean ± SD. **p < 0.01, Student's t-test.

The results in Nes-STAT3 and GFAP-STAT3 mice were not compared statistically due to differences in Tamoxifen treatment for their respective control mice. Nevertheless, the outcome of partial and selective PRA ablation in GFAP-STAT3 mice appears to be comparable to that of extensive and non-selective reactive astrocyte ablation in Nes-STAT3 mice. In addition, this exacerbation of injury was accompanied by a similarly increased inflammation and BBB disruption, as reflected by increases in perilesional CD68+ microglia (137% and 86% increases) and IgG deposition (368% and 221% increases), respectively. These results indicate that the incomplete accumulation of PRAs impairs wound healing by increasing inflammation and BBB disruption. In addition, tracing the fate of PRAs through selective reporter gene expression using *GFAP-CreER^{T2}* revealed that the majority of PRAs persisted as GFAP+ reactive astrocytes after wound healing and the reduction of PRAs. This suggests that PRAs are cleared after wound healing without contributing to the replenishment of brain cells as stem cells.

The present results showing the reporter gene expression in both neurons and astrocytes by *Nestin-Cre* is consistent with a number of studies using the same mouse strain. *Nestin-Cre* induces reporter gene expression in neural stem cells in both the developing spinal cord and brain (Dubois et al., 2006), and is widely used for ubiquitous reporter gene expression, as well as conditional knockout in the adult spinal cord and brain (Di Malta et al., 2012; Jia et al., 2016). We speculate that the reports showing the exclusive reporter gene expression in PRAs by *Nestin-Cre* after spinal cord injury (Okada et al., 2006; Renault-Mihara et al., 2017) may reflect additional reporter gene expression after injury and a more pronounced contrast than in the present study. This possibility arises because these studies utilized a reporter mouse strain carrying multiple copies of the reporter gene (Kawamoto et al., 2000). Thus, it is most likely that the deletion of *Stat3* occurred during development in some neurons and astrocytes, and then additionally in Nestin-expression reactive astrocytes after injury in both spinal cord (Okada et al., 2006; Renault-Mihara et al., 2017) and the present study. The deletion of Stat3 in neurons does not complicate the essential role of PRAs in wound healing, because STAT3 activation was limited in reactive astrocytes in both studies. Although GFAP is a pan marker of reactive astrocytes, *GFAP-CreERT2* selectively induced reporter gene expression in the PRAs after photo injury. Since the GFAP promoter contains AP-1 and SP-1 binding sites that are activated by growth signals (Brenner and Messing, 2021), it was likely further activated in the PRAs during proliferation (Gazon et al., 2018). Our experimental conditions including the dose and timing of tamoxifen treatment, mouse strain and method of injury, for the PRA selective recombination, will accelerate future studies of this protective reactive astrocyte subpopulation. In addition, this method is advantageous over the classical method for ablating proliferative reactive astrocytes by thymidine kinase expression by *Gfap* promoter and Ganciclovir treatment, which also ablate intestinal GFAP+ cells and cause death after long-term treatment (Bush et al., 1998).

The robust exacerbation by the partial PRA ablation likely implies that the PRAs are actively involved in wound healing by anti-inflammatory and regenerative functions, rather than by glial scar formation. Perilesional proliferation of reactive astrocytes is generally thought to form glial scar and isolate toxic substances and cells in the LC (Okada et al., 2006). However, the involvement of PRAs in glial scar formation is complicated by recent studies indicating the production of scar-forming reactive astrocytes by NG2 glia (Hesp et al., 2018; Kirdajova et al., 2021). In addition, a recent report showing the permeability of glial scar to toxic substances (Zbesko et al., 2018) raised a question about the protective function of glial scar. On the other hand, anti-inflammatory and regenerative functions characterize A2 reactive astrocytes, which share proliferation and Nestin expression with the PRAs (Liddelow et al., 2017). Among the anti-inflammatory cytokines produced by A2 reactive astrocytes (Luo, 2022), TGF-β not only suppresses inflammation, but also promotes tissue remodeling by inducing the production of extracellular matrix and tight junction proteins after various injuries (Lichtman et al., 2016). Indeed, the astrocyte-selective conditional knockout of TGF-β has been shown to cause severe infiltration of immune cells, including CD68+ microglia (Cekanaviciute et al., 2014) and to accelerate BBB disruption (Ronaldson et al., 2009). Thus, the PRAs are likely categorized as A2 reactive astrocytes and their ablation may exacerbate the injury by reducing TGF-β. However, the present study does not exclude the involvement of other reactive astrocytes-derived anti-inflammatory cytokines, such as IL-10 (Shanaki-Bavarsad et al., 2022) and tissue remodeling growth factors, such as Sonic hedgehog and VEGF (Argaw et al., 2012).

The clearance of PRA after wound healing is consistent with the report showing the reduction of A2 astrocytes after 14 dpi in ischemia model (Wang and Li, 2023). Resolution of gliosis, including clearance of activated astrocytes and microglia is important for avoiding chronic inflammation. However, its mechanisms, encompassing factors for intercellular communication, intracellular signaling, and glial cell fate are largely unknown. Although there have been reports of neuronal differentiation of Nestin-expressing reactive astrocytes after transfer to cell culture has been reported (Sirko et al., 2013), the PRA did

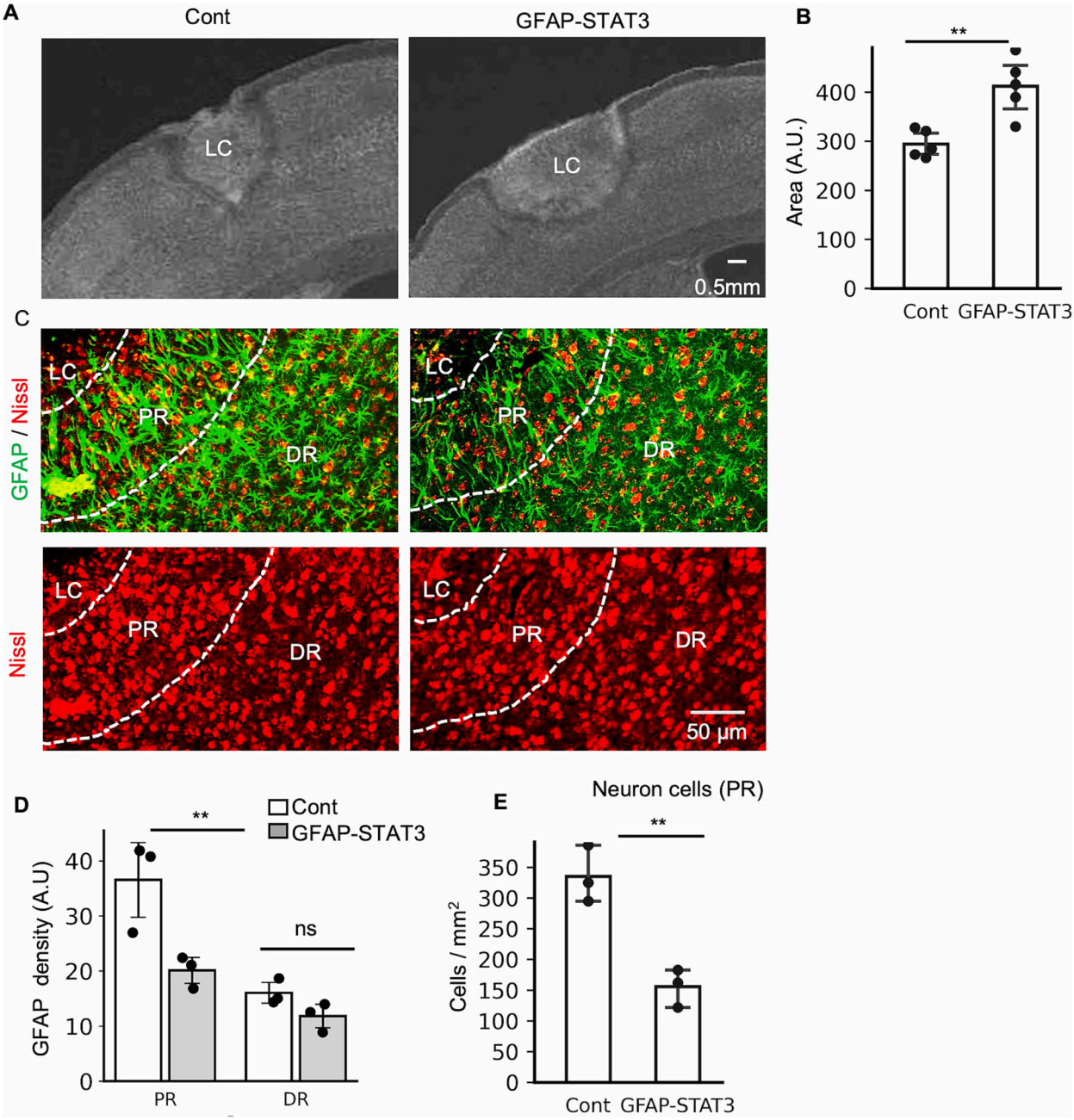

Fig. 7. The ablation of reactive astrocytes was accompanied by the increased of LC size and perilesional neuronal loss in GFAP-STAT3 mice.
Low magnification Nissl staining images of LC (A) and LC size (B) in Cont ($n = 5$) and *Gfap-CreER^{T2}:Stat3$^{f/f}$* (GFAP-STAT3, n = 5) mice at 7 dpi. High magnification images of GFAP+ immunostaining and Nissal+ staining (C) and the density of GFAP+ fibers in the PR and DR (D) and perilesional neuron (E) in tamoxifen-treated Cont (n = 3) and GFAP-STAT3 mice (n = 3) at 7 dpi. Mean ± SD. **p < 0.01, Student's t-test.

differentiate into non-astrocytic cells in the present study. Thus, the it is suggested that the lesion environment after closed head injury prevents the PRAs from differentiating into other cell types.

Our results suggest that the failure of PRA accumulation impairs the wound healing in patients with closed head injuries. Systemic and local inflammation are likely to inhibit the proliferation of PRAs, because our previous *in vitro* study showed the suppression of growth factor-induced astrocyte functions by proinflammatory cytokines (Morita et al., 2003) (Morita et al., 2007), and A2 reactive astrocytes are converted to A1 subtype by pro-inflammatory substances (Liddelow et al., 2017). Thus, the biochemical measurement of inflammatory factors and molecular imaging techniques, like PET and SPECT, tailored for PRAs, will emerge as a future diagnostic method for monitoring wound healing after closed head injury. In addition, the therapeutic treatment to ensure the balance in the accumulation and clearance of PRAs will improve the outcome of closed head injury. The excessive accumulation or impaired clearance of PRAs may hinder recovery. This is because some extracellular matrix proteins produced by reactive astrocytes for tissue remodeling, especially chondroitin sulfate proteoglycan are known to inhibit neurite growth during neuronal network reorganization (Bartus et al., 2012). Hence, both diagnostic and therapeutic strategies for PRAs should prioritize regulating their accumulation at an appropriate level.

The present results demonstrate the essential role of PRAs in wound healing after the photo injury. Meanwhile, the wound healing in patients with closed-head injury is often unpredictable due to various factors such as gender (Mollayeva et al., 2018), age (Coulter and Forsyth,

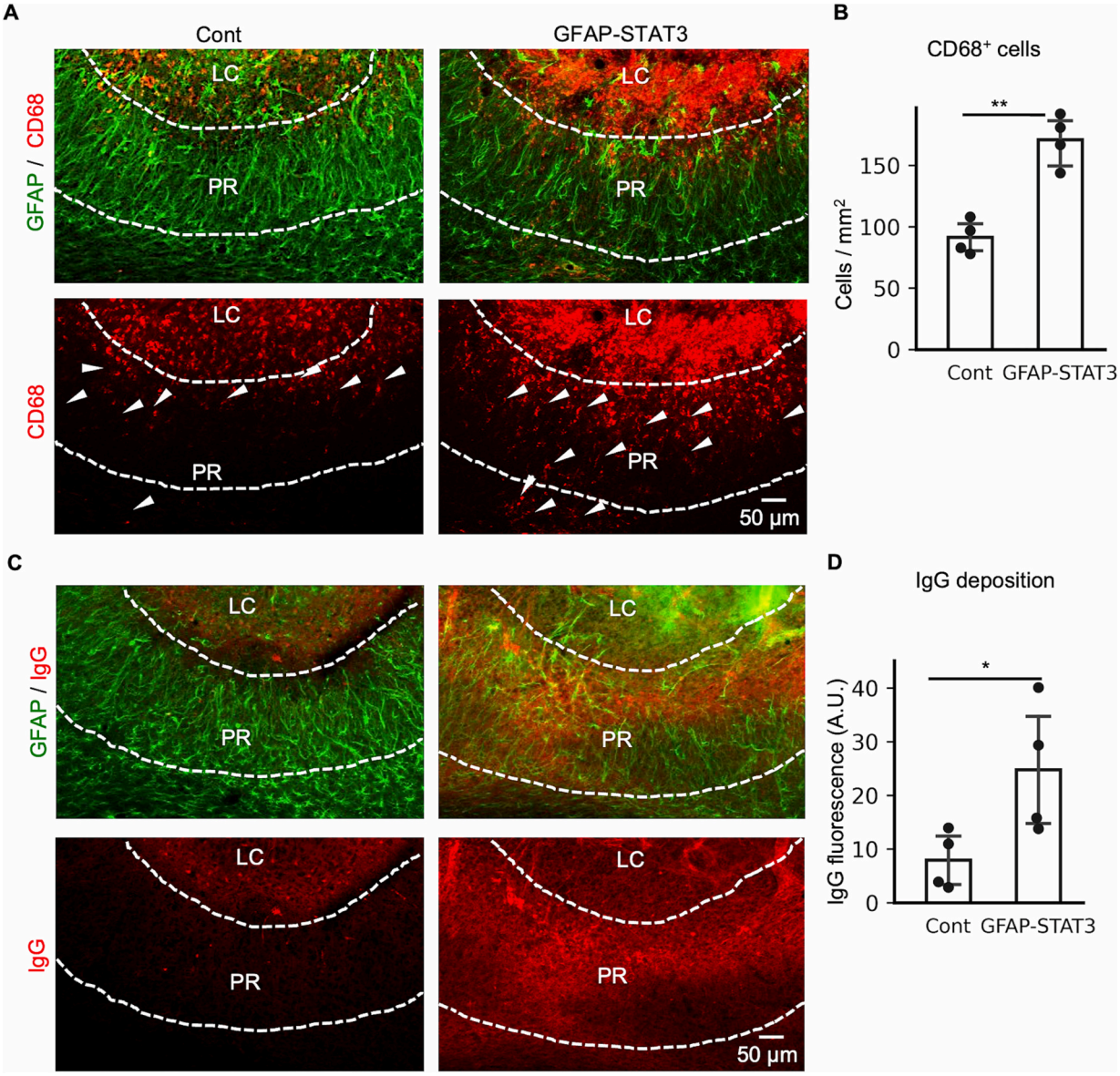

Fig. 8. Increased inflammation and BBB disruption in GFAP-STAT3 mice at 7 dpi.
GFAP and CD68 immunostaining images (A) and density of CD68+ cells in the PLR (B) in Cont (n = 4) and GFAP-STAT3 (n = 4) mice at 7 dpi. Arrowheads indicate CD68+ cells in the PR in (A). GFAP and IgG immunostaining images (C) and the intensity of IgG immunofluorescence in the PR in Cont (n = 4) and GFAP-STAT3 (n = 4) mice at 7 dpi. Mean ± SD. **p < 0.01, *P < 0.05, Student's t-test.

2019), genetic background (McAllister, 2015), nutritional status (Härtl et al., 2008), and medical history (Maas et al., 2017). Therefore, the clinical relevance of these findings will be further validated by analyzing the consequence of PRA ablation after the photo injury under various conditions. This study primarily focused on perilesional recovery at 7 dpi and demonstrated the protective effects of PRAs during the sub-acute phase of brain injury. Further long-term physiological and behavioral analysis of the photo injury will establish the contribution of PRAs to the outcome of closed-head injury. The PRAs shared a number of characteristics with A2 reactive astrocytes. The single-cell gene expression profiles of reactive astrocytes after the photo injury are expected to identify the PRAs as A2 reactive astrocytes and propose the photo injury as an experiment model for studying the role of A2 reactive astrocytes in wound healing. The gene expression profile may also reveal previously uncategorized subpopulations of reactive astrocytes in the distal region of the photo injury. Beyond the categorization of A1 and A2, recent proposals emphasize the importance of assessing reactive astrocytes *in vivo* using multiple molecular and functional parameters (Escartin et al., 2021). The distal reactive astrocytes differ from the PRAs in terms of proliferation and Nestin expression, while lacking the neurotoxic influences of A1 reactive astrocytes (Suzuki et al., 2012). In addition, the gene expression profile will address the mechanisms regulating the accumulation of PRA, as well as the anti-inflammatory and tissue repair functions of PRA, and lead to diagnosis and therapeutic advancement based on this study to improve the outcome of closed head injury.

Funding sources

This work was supported by JSPS/MEXT KAKENHI Grant Number 23300133, 23122513 and 18KT0071.

Declaration of generative AI and AI-assisted technologies in the writing process

During the preparation of this work the author(s) used ChatGPT 3.5

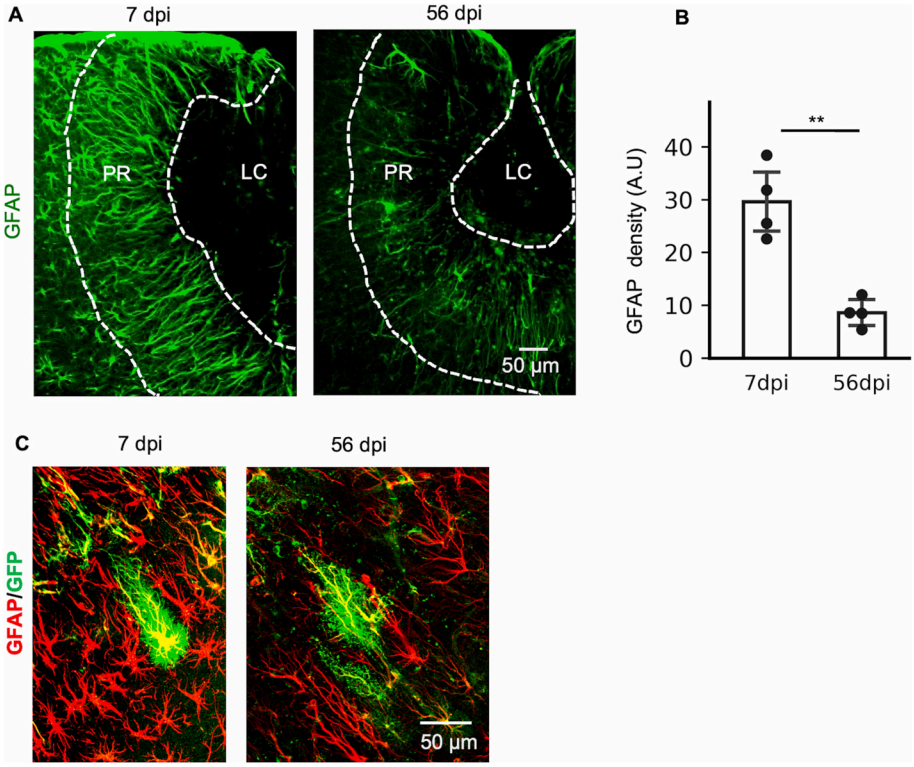

Fig. 9. Elimination of RPAs after wound healing.
GFAP immunostaining images (A) and the density of GFAP+ fibers in the PR (B) of GFAP-GCaMP mice at 7 dpi (n = 4) and 56 dpi (n = 4). GFP and GFAP immunostaining images of PRAs at 7 dpi and 56 dpi (C). mean ± SD. **p < 0.01, Student's t-test.

in order to improve English. After using this tool/service, the author(s) reviewed and edited the content as needed and take(s) full responsibility for the content of the publication.

CRediT authorship contribution statement

Nitin Sawant: Writing – original draft, Visualization, Investigation. **Airi Watanabe:** Visualization, Investigation. **Haruna Ueda:** Visualization, Investigation. **Hideyuki Okano:** Writing – review & editing, Resources, Funding acquisition, Conceptualization. **Mitsuhiro Morita:** Writing – review & editing, Validation, Supervision, Project administration, Funding acquisition, Conceptualization.

Declaration of competing interest

The authors declare no conflict of interest.

Data availability

The data support the findings of this study are available from the corresponding author upon reasonable request.

References

Amorini, A.M., Lazzarino, G., Di Pietro, V., Signoretti, S., Lazzarino, G., Belli, A., Tavazzi, B., 2016. Metabolic, enzymatic and gene involvement in cerebral glucose dysmetabolism after traumatic brain injury. Biochim. Biophys. Acta (BBA) - Mol. Basis Dis. 1862, 679–687.

Argaw, A.T., Asp, L., Zhang, J., Navrazhina, K., Pham, T., Mariani, J.N., Mahase, S., Dutta, D.J., Seto, J., Kramer, E.G., Ferrara, N., Sofroniew, M.V., John, G.R., 2012. Astrocyte-derived VEGF-A drives blood-brain barrier disruption in CNS inflammatory disease. J. Clin. Invest. 122, 2454–2468.

Bartus, K., James, N.D., Bosch, K.D., Bradbury, E.J., 2012. Chondroitin sulphate proteoglycans: key modulators of spinal cord and brain plasticity. Exp. Neurol. 235, 5–17.

Brenner, M., Messing, A., 2021. Regulation of GFAP expression. ASN Neuro 13, 1759091420981206.

Bush, T.G., Savidge, T.C., Freeman, T.C., Cox, H.J., Campbell, E.A., Mucke, L., Johnson, M.H., Sofroniew, M.V., 1998. Fulminant jejuno-ileitis following ablation of enteric glia in adult transgenic mice. Cell 93, 189–201.

Cekanaviciute, E., Dietrich, H.K., Axtell, R.C., Williams, A.M., Egusquiza, R., Wai, K.M., Koshy, A.A., Buckwalter, M.S., 2014. Astrocytic TGF-β signaling limits inflammation and reduces neuronal damage during central nervous system *toxoplasma* infection. J. Immunol. 193, 139–149.

Chen, C., Zhong, X., Smith, D.K., Tai, W., Yang, J., Zou, Y., Wang, L.-L., Sun, J., Qin, S., Zhang, C.-L., 2019. Astrocyte-specific deletion of Sox2 promotes functional recovery after traumatic brain injury. Cereb. Cortex 29, 54–69.

Coulter, I.C., Forsyth, R.J., 2019. Paediatric traumatic brain injury. Curr. Opin. Pediatr. 31, 769–774.

Das, A., Smith, M.A., O'Dowd, D.K., 2021. A behavioral screen for heat-induced seizures in mouse models of epilepsy. J. Vis. Exp.

Di Malta, C., Fryer, J.D., Settembre, C., Ballabio, A., 2012. Astrocyte dysfunction triggers neurodegeneration in a lysosomal storage disorder. Proc. Natl. Acad. Sci. USA 109. https://doi.org/10.1073/pnas.1209577109. Available at:. [Accessed October 3, 2023].

Dubois, N.C., Hofmann, D., Kaloulis, K., Bishop, J. m., Trumpp, A., 2006. Nestin-Cre transgenic mouse line Nes-Cre1 mediates highly efficient Cre/loxP mediated recombination in the nervous system, kidney, and somite-derived tissues. Genesis 44, 355–360.

Escartin, C., et al., 2021. Reactive astrocyte nomenclature, definitions, and future directions. Nat. Neurosci. 24, 312–325.

Fan, Y.-Y., Huo, J., 2021. A1/A2 astrocytes in central nervous system injuries and diseases: angels or devils? Neurochem. Int. 148, 105080.

Gavériaux-Ruff, C., Kieffer, B.L., 2007. Conditional gene targeting in the mouse nervous system: insights into brain function and diseases. Pharmacol. Ther. 113, 619–634.

Gazon, H., Barbeau, B., Mesnard, J.-M., Peloponese, J.-M., 2018. Hijacking of the AP-1 signaling pathway during development of ATL. Front. Microbiol. 8 https://doi.org/10.3389/fmicb.2017.02686. Available at:. [Accessed October 3, 2023].

Götz, M., Sirko, S., Beckers, J., Irmler, M., 2015. Reactive astrocytes as neural stem or progenitor cells: in vivo lineage, in vitro potential, and genome-wide expression analysis. Glia 63, 1452–1468.

Harlow, E., Lane, D., 2006. Mounting samples in gelvatol or mowiol. Cold Spring Harb Protoc. https://cshprotocols.cshlp.org/content/2006/1/pdb.prot4461.

Härtl, R., Gerber, L.M., Ni, Q., Ghajar, J., 2008. Effect of early nutrition on deaths due to severe traumatic brain injury. J. Neurosurg. 109, 50–56.

Herrmann, J.E., Imura, T., Song, B., Qi, J., Ao, Y., Nguyen, T.K., Korsak, R.A., Takeda, K., Akira, S., Sofroniew, M.V., 2008. STAT3 is a critical regulator of astrogliosis and scar formation after spinal cord injury. J. Neurosci. 28, 7231–7243.

Hesp, Z.C., Yoseph, R.Y., Suzuki, R., Jukkola, P., Wilson, C., Nishiyama, A., McTigue, D. M., 2018. Proliferating NG2-cell-dependent angiogenesis and scar formation alter

axon growth and functional recovery after spinal cord injury in mice. J. Neurosci. 38, 1366–1382.
Hirrlinger, P.G., Scheller, A., Braun, C., Hirrlinger, J., Kirchhoff, F., 2006. Temporal control of gene recombination in astrocytes by transgenic expression of the tamoxifen-inducible DNA recombinase variant CreERT2. Glia 54, 11–20.
Hunter, J.D., 2007. Matplotlib: a 2D graphics environment. Comput. Sci. Eng. 9, 90–95.
Jia, J., Lin, X., Lin, X., Lin, T., Chen, B., Hao, W., Cheng, Y., Liu, Y., Dian, M., Yao, K., Xiao, D., Gu, W., 2016. R/L, a double reporter mouse line that expresses luciferase gene upon Cre-mediated excision, followed by inactivation of mRFP expression. Genome 59, 816–827.
Kawamoto, S., Niwa, H., Tashiro, F., Sano, S., Kondoh, G., Takeda, J., Tabayashi, K., Miyazaki, J., 2000. A novel reporter mouse strain that expresses enhanced green fluorescent protein upon Cre-mediated recombination. FEBS Lett. 470, 263–268.
Kirdajova, D., Valihrach, L., Valny, M., Kriska, J., Krocianova, D., Benesova, S., Abaffy, P., Zucha, D., Klassen, R., Kolenicova, D., Honsa, P., Kubista, M., Anderova, M., 2021. Transient astrocyte-like NG2 glia subpopulation emerges solely following permanent brain ischemia. Glia 69, 2658–2681.
Koenig, J.B., Dulla, C.G., 2018. Dysregulated glucose metabolism as a therapeutic target to reduce post-traumatic epilepsy. Front. Cell. Neurosci. 12. Available at: https://doi.org/10.3389/fncel.2018.00350 [Accessed November 25, 2023].
Lichtman, M.K., Otero-Vinas, M., Falanga, V., 2016. Transforming growth factor beta (TGF-β) isoforms in wound healing and fibrosis. Wound Repair Regen. 24, 215–222.
Liddelow, S.A., et al., 2017. Neurotoxic reactive astrocytes are induced by activated microglia. Nature 541, 481–487.
Luo, J., 2022. TGF-β as a key modulator of astrocyte reactivity: disease relevance and therapeutic implications. Biomedicines 10, 1206.
Maas, A.I.R., et al., 2017. Traumatic brain injury: integrated approaches to improve prevention, clinical care, and research. Lancet Neurol. 16, 987–1048.
McAllister, T.W., 2015. Genetic factors in traumatic brain injury. Handb. Clin. Neurol. 128, 723–739.
Mollayeva, T., Mollayeva, S., Colantonio, A., 2018. Traumatic brain injury: sex, gender and intersecting vulnerabilities. Nat. Rev. Neurol. 14, 711–722.
Morita, M., Higuchi, C., Moto, T., Kozuka, N., Susuki, J., Itofusa, R., Yamashita, J., Kudo, Y., 2003. Dual regulation of calcium oscillation in astrocytes by growth factors and pro-inflammatory cytokines via the mitogen-activated protein kinase cascade. J. Neurosci. 23, 10944–10952.
Morita, M., Saruta, C., Kozuka, N., Okubo, Y., Itakura, M., Takahashi, M., Kudo, Y., 2007. Dual regulation of astrocyte gap junction hemichannels by growth factors and a pro-inflammatory cytokine via the mitogen-activated protein kinase cascade. Glia 55, 508–515.
Myer, D.J., Gurkoff, G.G., Lee, S.M., Hovda, D.A., Sofroniew, M.V., 2006. Essential protective roles of reactive astrocytes in traumatic brain injury. Brain 129, 2761–2772.
Nobuta, H., Ghiani, C.A., Paez, P.M., Spreuer, V., Dong, H., Korsak, R.A., Manukyan, A., Li, J., Vinters, H.V., Huang, E.J., Rowitch, D.H., Sofroniew, M.V., Campagnoni, A.T., de Vellis, J., Waschek, J.A., 2012. STAT3-mediated astrogliosis protects myelin development in neonatal brain injury. Ann. Neurol. 72, 750–765.
Ohkura, M., Sasaki, T., Sadakari, J., Gengyo-Ando, K., Kagawa-Nagamura, Y., Kobayashi, C., Ikegaya, Y., Nakai, J., 2012. Genetically encoded green fluorescent Ca2+ indicators with improved detectability for neuronal Ca2+ signals. PLoS One 7, e51286.
Okada, S., Nakamura, M., Katoh, H., Miyao, T., Shimazaki, T., Ishii, K., Yamane, J., Yoshimura, A., Iwamoto, Y., Toyama, Y., Okano, H., 2006. Conditional ablation of Stat3 or Socs3 discloses a dual role for reactive astrocytes after spinal cord injury. Nat. Med. 12, 829–834.
Reichenbach, N., Delekate, A., Plescher, M., Schmitt, F., Krauss, S., Blank, N., Halle, A., Petzold, G.C., 2019. Inhibition of Stat3-mediated astrogliosis ameliorates pathology in an Alzheimer's disease model. EMBO Mol. Med. 11, e9665.
Renault-Mihara, F., Mukaino, M., Shinozaki, M., Kumamaru, H., Kawase, S., Baudoux, M., Ishibashi, T., Kawabata, S., Nishiyama, Y., Sugai, K., Yasutake, K., Okada, S., Nakamura, M., Okano, H., 2017. Regulation of RhoA by STAT3 coordinates glial scar formation. J. Cell Biol. 216, 2533–2550.
Ronaldson, P.T., DeMarco, K.M., Sanchez-Covarrubias, L., Solinsky, C.M., Davis, T.P., 2009. Transforming growth factor-β signaling alters substrate permeability and tight junction protein expression at the blood-brain barrier during inflammatory pain. J. Cereb. Blood Flow Metab. 29, 1084–1098.
Schindelin, J., Arganda-Carreras, I., Frise, E., Kaynig, V., Longair, M., Pietzsch, T., Preibisch, S., Rueden, C., Saalfeld, S., Schmid, B., Tinevez, J.-Y., White, D.J., Hartenstein, V., Eliceiri, K., Tomancak, P., Cardona, A., 2012. Fiji: an open-source platform for biological-image analysis. Nat. Methods 9, 676–682.
Shanaki-Bavarsad, M., Almolda, B., González, B., Castellano, B., 2022. Astrocyte-targeted overproduction of IL-10 reduces neurodegeneration after TBI. Exp. Neurobiol. 31, 173–195.
Sirko, S., et al., 2013. Reactive glia in the injured brain acquire stem cell properties in response to sonic hedgehog. Cell Stem Cell 12, 426–439.
Suzuki, T., Sakata, H., Kato, C., Connor, J.A., Morita, M., 2012. Astrocyte activation and wound healing in intact-skull mouse after focal brain injury. Eur. J. Neurosci. 36, 3653–3664.
Wang, C., Li, L., 2023. The critical role of KLF4 in regulating the activation of A1/A2 reactive astrocytes following ischemic stroke. J. Neuroinflammation 20, 44.
Xu, H.-T., Pan, F., Yang, G., Gan, W.-B., 2007. Choice of cranial window type for in vivo imaging affects dendritic spine turnover in the cortex. Nat. Neurosci. 10, 549–551.
Zbesko, J.C., Nguyen, T.-V.V., Yang, T., Frye, J.B., Hussain, O., Hayes, M., Chung, A., Day, W.A., Stepanovic, K., Krumberger, M., Mona, J., Longo, F.M., Doyle, K.P., 2018. Glial scars are permeable to the neurotoxic environment of chronic stroke infarcts. Neurobiol. Dis. 112, 63–78.